Biophysical Journal Volume 86 March 2004 1263–1269

Effects of Intermediate Bound States in Dynamic Force Spectroscopy

Imre Derényi,* Denis Bartolo,† and Armand Ajdari†
*Department of Biological Physics, Eötvös University, H-1117 Budapest, Hungary; and †Laboratoire de Physico-Chimie Théorique, UMR 7083 CNRS, Ecole Supérieure de Physique et de Chimie Industrielles, F-75231 Paris Cédex 05, France

ABSTRACT We revisit some aspects of the interpretation of dynamic force spectroscopy experiments. The standard theory predicts that the typical unbinding force f^* is linearly proportional to the logarithm of the loading rate r when a single energy barrier controls the unbinding process. For a more complex situation of N barriers, it predicts at most N linear segments for the f^* vs. $\log(r)$ curve, each segment characterizing a different barrier. Here we extend this existing picture using a refined approximation, provide a more general analytical formula, and show that in principle up to $N(N + 1) / 2$ segments can show up experimentally. As a consequence, the determination of the positions and even the number of the energy barriers from the experimental data can be ambiguous. A further possible consequence of a multiple-barrier landscape is a bimodal or multimodal distribution of the unbinding force at certain loading rates, a feature recently observed experimentally.

INTRODUCTION

The last decades have witnessed a revolution in the methods to observe and manipulate single biomacromolecules or biomolecule complexes. New micromanipulation techniques have especially been put forward to probe the folded structure of proteins and to quantify the strength of adhesion complexes (Kellermayer et al., 1997; Nishizaka et al., 2000; Pierres et al., 1996; Poirier et al., 2001; Rief et al., 1997; Simson et al., 1999; Strick et al., 2003; Weisel et al., 2003). An important step in this direction is the proposal of the Evans group to use soft structures to pull on adhesion complexes or molecules at various loading rates (dynamic force spectroscopy) (Evans and Ritchie, 1997; Merkel et al., 1999). Moving the other end of the soft structure at constant velocity induces on the complex a pulling force that increases linearly in time $f = rt$. Measuring the typical unbinding time t^* yields an unbinding force $f^* = rt^*$ that depends on the pulling rate r. The typical outcome of such experiments is a plot of f^* vs. $\log(r)$ (force spectrum) composed of a succession of straight lines with increasing slopes. It has been argued that it is possible to deduce the values of some relevant structural parameters of the complex by analyzing the force spectrum, thanks to an adiabatic Kramers picture. In this picture the unbinding process is considered as a thermally activated escape from bound states over a succession of barriers along a one-dimensional (1D) path of a mountainous energy landscape (Evans and Ritchie, 1997; Merkel et al., 1999). Within this scheme, each straight line of the force spectrum witnesses the overcome of an energy barrier, and its slope maps the barrier to a distance x along the pulling direction. This procedure has been shown to yield reasonable values for a few systems, and has been confirmed by numerical simulations (Grubmüller et al., 1996).

Subsequently, theoretical studies have refined the above original model, e.g., by inclusion of rebinding events (Seifert, 2002); study of time-dependent loading rates (Evans and Ritchie, 1997; Merkel et al., 1999); incorporation of more details of the shape of the energy wells, energy barriers, and loading potential (Hummer and Szabo, 2003; Seifert, 2002); or consideration of more complex topographies (Strunz et al., 2000) and topologies of the energy landscape (Bartolo et al., 2002).

In this article we explore the potential influence of the existence of intermediate bound states on the experimental dynamic response of adhesion complexes as probed in dynamic force spectroscopy. To achieve this goal, we first revisit the analysis of the escape from a bound state consisting of an arbitrary number of barriers along a 1D path under the application of an external load (in line with earlier studies of Strunz et al. (2000)), and then discuss the implications of this analysis for the interpretation of experimental data. In the third section (''Stochastic kinetics of unbinding under external forces. . .''), the standard picture is recalled, together with its two underlying assumptions. In the fourth section (''Beyond the deeply bound fundamental state approximation''), we first relax the a priori assumption of a deep fundamental bound state and provide a general expression that relates the typical rupture force to the loading rate (within a single escape rate approximation). The practical implications of this new formula (Eq. 15) are discussed, and in particular we comment upon intrinsic ambiguities in inferring information from a $[\log(r), f^*]$ plot. Then we show in the final section (''Beyond the single escape rate approximation. . .'') that in the presence of multiple bound states it may be necessary to relax the other assumption (a single typical rupture force for each loading rate) as multimodal rupture force distributions naturally show up, a feature recently observed in lipid extraction experiments (Evans and Williams, 2002).

Submitted July 17, 2003, and accepted for publication September 25, 2003.
Address reprint requests to Imre Derényi, Dept. of Biological Physics, Eötvös University, Pázmány P. Stny. 1A, H-1117 Budapest, Hungary. E-mail: derenyi@elte.hu.

0006-3495/04/03/1263/07 $2.00

MODEL AND NOTATIONS

Fig. 1 illustrates the energy landscape of a one-dimensional escape path with N energy barriers and wells. The position and energy of the ith energy well ($i = 0$ marking the fundamental bound state, and $1 \le i \le N-1$ the intermediate ones) are denoted by x_i and E_i, respectively. Similarly, the position and energy of the jth energy barrier are denoted by $\hat{x}_j$ and $\hat{E}_j$, respectively (where $1 \le j \le N$). For convenience, without losing generality, we set $x_0 = 0$ and $E_0 = 0$ for the fundamental bound state. The unbound ''state'' is on the right-hand side of the Nth barrier. If the energy differences $(\hat{E}_i - E_i)$ and $(\hat{E}_{i+1} - E_i)$ exceed k_BT the transition rates k_i^- (and k_i^+) from the ith energy well over the left ith barrier (and right $(i+1)$th barrier, respectively) can be written according to the Kramers formula

$$k_i^- = \omega_0 \alpha_i \hat{\alpha}_i e^{-(\hat{E}_i - E_i)/k_BT}, \quad (1)$$

$$k_i^+ = \omega_0 \alpha_i \hat{\alpha}_{i+1} e^{-(\hat{E}_{i+1} - E_i)/k_BT}, \quad (2)$$

where ω_0 is a typical attempt frequency, α_i and $\hat{\alpha}_j$ are geometric factors characterizing the shape of the ith energy well and jth energy barrier, respectively. Note that there is no transition from the fundamental bound state to the left, therefore, $k_0^- \equiv 0$.

We assume throughout the paper that the energy wells and barriers are sharp, so that for any loading force f their locations remain constant, and their energies change as $E_i(f) = E_i(0) - fx_i$ and $\hat{E}_j(f) = \hat{E}_j(0) - f\hat{x}_j$. To simplify the notations, wherever the argument of the energies and transition rates is omitted, a loading force f is implicitly assumed.

Finally it will prove convenient to introduce a few compact notations. For any $0 \le i < j \le N$ we denote the distance between the ith well and the jth barrier (on the right) by $\Delta x_{i,j} = \hat{x}_j - x_i$, and their energy difference by $\Delta E_{i,j} = \hat{E}_j - E_i$. We also define a formal (effective) rate constant from the ith well over the jth barrier on the right as

$$k_{i,j} = \omega_0 \alpha_i \hat{\alpha}_j e^{-\Delta E_{i,j}/k_BT}. \quad (3)$$

Obviously $\Delta E_{i,j}$ and $k_{i,j}$ implicitly depend on f, whereas $\Delta x_{i,j}$ are constants given the assumption of the previous paragraph.

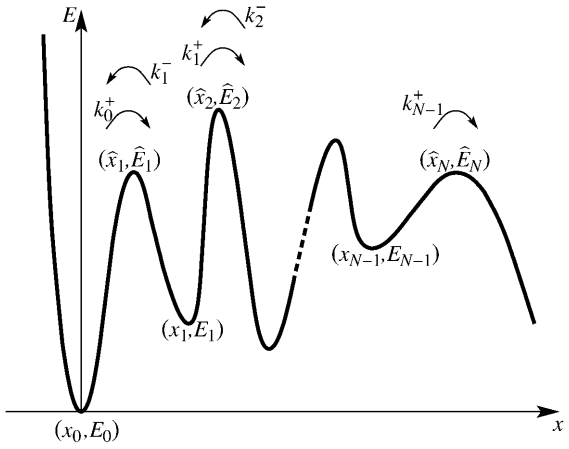

FIGURE 1 Sketch of the one-dimensional energy landscape describing the unbinding pathway projected along the pulling direction.

STOCHASTIC KINETICS OF UNBINDING UNDER EXTERNAL FORCES: STANDARD DESCRIPTION AND CORRESPONDING APPROXIMATIONS

We first recall the standard description of the ''force spectrum,'' which relies on two major assumptions, namely the single escape rate and the deeply bound fundamental state (DBFS) approximations.

Single escape rate approximation

If for any experimentally relevant load f the equilibration within the bound states is much faster than the escape to the unbound state, the unbinding can be described by a single load-dependent escape rate $k(f)$. Following the calculation of Evans (1998, 2001), if rebinding is negligible (which is the case in most experimental situations), the probability $P(t)$ of remaining in the bound state at time t (the survival probability of the bond) then decreases as

$$\frac{dP(t)}{dt} = -k(rt)P(t). \quad (4)$$

The solution of this differential equation is $P(t) = \exp[-\int_0^t k(rt')dt']$. The probability density for unbinding between times t and $t + \Delta t$ is $p_t(t) = -dP(t)/dt = k(rt)P(t)$, from which, after changing the variable from t to f, one gets the probability density for the distribution of the unbinding force: $p_f(f) = (1/r)k(f)P(f/r)$. The typical unbinding force f^* is defined as the peak of this probability density: $dp_f(f)/df|_{f=f^*} = 0$, which yields the simple formula

$$\left.\frac{d\tau(f)}{df}\right|_{f=f^*} = -\frac{1}{r}, \quad (5)$$

where $\tau(f) \equiv 1/k(f)$ denotes the load-dependent mean escape time. This formula gives the loading rate r at which the typical unbinding force is f^*. For practical purposes it is often necessary to invert this relation to, e.g., predict the typical unbinding force for an experimentally imposed loading rate.

To set a reference for further comparison, we explicitly invert the above relation in case of a single barrier, i.e., when $\tau(f) = \tau(0)\exp(-f\hat{x}_1)$, and obtain

$$f^* = \frac{k_BT}{\hat{x}_1} \ln\left[\frac{r\tau(0)\hat{x}_1}{k_BT}\right]. \quad (6)$$

As mentioned in the introduction, the escape over a single barrier results in a single straight line in the force spectrum. The experimental observation of a linear segment consequently gives hints as to the structure of the energy landscape, in particular the slope of the segment permits to deduce a distance $\hat{x}_1$ between the energy well and the barrier.

Deeply bound fundamental state approximation

Assuming further that the fundamental bound state is much deeper than the intermediate ones: $E_i(f) - E_0(f) \gg k_BT$ for any experimentally relevant load f (i.e., before unbinding has statistically almost certainly occurred; see Fig. 2 *a*.), Evans (1998, 2001) and Evans and Williams (2002) have shown that the mean escape time from the fundamental bound state to the unbound state is well approximated by Evans (1998, 2001) and Evans and Williams (2002)

$$\tau(f) = \sum_{j=1}^{N} \frac{1}{k_{0,j}(f)} = \sum_{j=1}^{N} \frac{e^{-f\Delta x_{0,j}/k_BT}}{k_{0,j}(0)}. \quad (7)$$

This allows one to obtain an explicit r vs. f^* relationship by plugging Eq. 7 into Eq. 5, which yields the compact formula

$$r = \left[\sum_{j=1}^{N} \frac{\Delta x_{0,j}}{k_BT} \frac{e^{-f^*\Delta x_{0,j}/k_BT}}{k_{0,j}(0)} \right]^{-1}. \quad (8)$$

This equation predicts a spectrum f^* vs. $\log(r)$ consisting of a succession of at most N segments of increasing slopes, each of which yielding an information $\Delta x_{0,j}$ about an intermediate barrier.

BEYOND THE DEEPLY BOUND FUNDAMENTAL STATE APPROXIMATION

In this section we relax the DBFS approximation, generalize Eqs. 7 and 9 accordingly, and discuss the experimental implications of this generalization.

Refined theory

In general, it is possible that for large enough forces one or more of the intermediate bound states become deeper than the fundamental bound state before unbinding has occurred (see Fig. 2 *b*). In such cases the above DBFS approximation breaks down. However, we show below that it is still possible to compute rather simply the escape time τ from the ''bound state'' to the ''unbound state,'' provided we maintain the assumption of a single escape rate $1/\tau(f)$.

Let us put the system into its fundamental bound state, and let it evolve according to the transition rates given in Eqs. 1 and 2. Whenever the system gets into the unbound state (by making a transition over the outermost barrier) let us place it back into the fundamental bound state. The stationary state of an ensemble of such systems is characterized by a probability current, which is constant everywhere and equal to $1/\tau$ by definition. To calculate τ we have to solve the following system of equations:

$$P_i k_i^+ - P_{i+1} k_{i+1}^- = 1/\tau \quad 0 \le i \le N-2, \quad (9)$$

$$P_{N-1} k_{N-1}^+ = 1/\tau, \quad (10)$$

$$\sum_{i=0}^{N-1} P_i = 1, \quad (11)$$

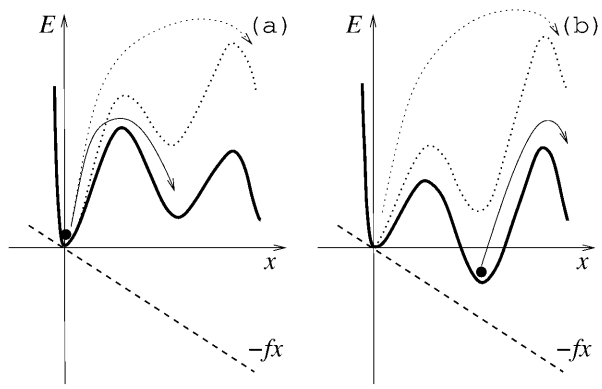

FIGURE 2 Sketch of two energy landscapes with one intermediate well. Dotted drawings: no external force. When a constant force is applied, energies are lowered by fx (*dashed lines*); the resulting landscapes appear in solid lines. The dotted arrows indicate which pair of wells and barriers control the kinetics at zero load. The solid arrows indicate the new limiting effective escape process at higher forces. (*a*) The escape from the fundamental bound state remains the limiting process whatever the pulling force. (*b*) The escape from the intermediate bound state energy becomes the limiting process at high forces.

where P_i denotes the probability of being in the ith bound state ($0 \le i \le N-1$). The first N equations describe the probability current over each of the N barriers, and the last equation is just the normalization condition. These $N+1$ linear equations uniquely determine the $N+1$ variables (P_i and τ), and can be solved easily in a recursive way. First, $P_{N-1}\tau$ can be expressed from Eq. 10, and then $P_{N-2}\tau, \ldots,$ $P_0\tau$ recursively from Eq. 9 yielding

$$P_i\tau = \frac{1}{k_i^+} + \frac{k_{i+1}^-}{k_i^+ k_{i+1}^+} + \ldots + \frac{k_{i+1}^- \ldots k_{N-1}^-}{k_i^+ k_{i+1}^+ \ldots k_{N-1}^+} = \sum_{j=i+1}^{N} \frac{1}{k_{i,j}}, \quad (12)$$

where Eqs. 1, 2, and the definition (Eq. 3) have been used. Note that because the $k_{i,j}$ are only formal definitions, constructed as products and ratios of the single-barrier rates (Eq. 1) and (Eq. 2), they are meaningful even if $\Delta E_{i,j} < 0$. From the normalization (Eq. 11) one can easily express τ as

$$\tau = \sum_{i=0}^{N-1} P_i\tau = \sum_{i=0}^{N-1} \sum_{j=i+1}^{N} \frac{1}{k_{i,j}}. \quad (13)$$

The sum is dominated by the smallest effective rates, which are the bottlenecks of the unbinding process. Consequently, this formula remains a good approximation for τ even if some of the barriers disappear at big loads, because the corresponding formal transition rates make negligible contributions. By indicating the load force f explicitly, we arrive at

$$\tau(f) = \sum_{i=0}^{N-1} \sum_{j=i+1}^{N} \frac{1}{k_{i,j}(f)} = \sum_{i=0}^{N-1} \sum_{j=i+1}^{N} \frac{e^{-f\Delta x_{i,j}/k_BT}}{k_{i,j}(0)}, \quad (14)$$

which generalizes Eq. 7. An analytic formula can be given for the f^* vs. r relationship by plugging Eq. 14 into Eq. 5:

$$r = \left[\sum_{i=0}^{N-1} \sum_{j=i+1}^{N} \frac{\Delta x_{i,j}}{k_B T} \frac{e^{-f^* \Delta x_{i,j}/k_B T}}{k_{i,j}(0)} \right]^{-1}. \quad (15)$$

This generalization of Eq. 8 is one of the main results of this paper. Let us briefly comment on immediate features of this new formula.

First, Eq. 8 is easily recovered from Eq. 15 assuming a DBFS. Indeed, the assumption $E_i(f) \gg E_0(f)$ implies $k_{0,j} \gg k_{i,j}$, if $i > 0$ (see Eq. 3) and therefore, the relation $P_i/P_0 \ll 1$, if $i > 0$ is deduced from Eq. 12. The probability to find the system in the fundamental bound state is close to 1. So, the sum over i in Eq. 14 is dominated by the contributions of the effective escape rates from the 0th well only. Finally, the sum over i (labeling the intermediate states) is reduced to its sole first term too, and Eq. 15 becomes identical to Eq. 8.

Second, each of the $N(N + 1) / 2$ terms of Eq. 15 alone would yield a straight line in the f^* vs. $\log(r)$ plot. However, at any loading rate the highest force value (the uppermost line, corresponding to the most difficult transition) limits the unbinding process, therefore, the $f^*(r)$ curve is expected to closely follow the upper envelope of these lines (see Fig. 3 *a*). Depending on the position of the lines, the upper envelope can consist of up to $N(N + 1) / 2$ linear segments.

Third, this last point is clearly at odds with the predictions of the DBFS approximation. Indeed, assuming a DBFS, one arrives at Evans' original result with a maximum of N linear segments, and all the remaining $N(N - 1) / 2$ segments, corresponding to the escape from the intermediate bound states, disappear.

Practical implications: ambiguity in the determination of "structural" parameters

We now insist on some practical implications of the above general description. We do not attempt a full inspection of all the possible dynamic responses of arbitrarily complex systems, but rather focus on two simple examples to stress that the main features of the energy landscape can in general not be unambiguously inferred from [$\log(r)$, f^*] plots. To emphasize the experimental relevance of this discussion, we use for the parameters values comparable to those observed in experimental systems. Specifically, we take the geometric factors α_i and $\hat{\alpha}_j$ values to be all equal to 1, $\omega_0 = 10^8\ s^{-1}$ and $k_B T = 4 \times 10^{-21}$ J.

Ambiguity in determining the barriers positions

Fig. 3, *a* and *b*, display two force spectra as obtained from Eq. 15. Both correspond to energy landscapes with two barriers. Though the two [$\log(r)$, f^*] plots are almost identical they are related to very different sets of values for the energy levels and positions (along the pulling direction) of the wells and the barriers.

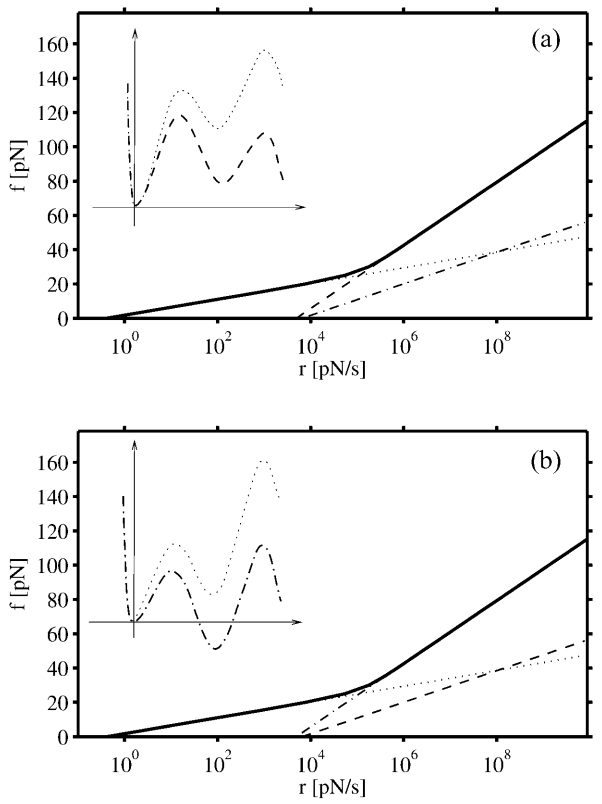

FIGURE 3 Two very similar force spectra corresponding to different energy landscapes with one intermediate well. Curves in solid lines: force spectra plotted using Eq. 15. It closely follows the upper envelope of the straight lines corresponding to the transitions: $k_{0,2}$ (*dotted line*), $k_{0,1}$ (*dashed line*), and $k_{1,2}$ (*dash-dotted line*). Insets: shape of the energy landscapes at low and high forces, each drawn with the same line style as the straight line associated with the limiting transition. Parameter values: (*a*) $(\hat{x}_1, \hat{E}_1) = (1\,\text{nm}, 11\,k_B T)$, $(x_1, E_1) = (1.5\ \text{nm}, 8\ k_B T)$, and $(\hat{x}_2, \hat{E}_2) = (2\,\text{nm}, 20\,k_B T)$; (*b*) $(\hat{x}_1, \hat{E}_1) = (0.5\,\text{nm}, 12\,k_B T)$, $(x_1, E_1) = (1\ \text{nm}, 9\ k_B T)$, and $(\hat{x}_2, \hat{E}_2) = (2\,\text{nm}, 20\,k_B T)$.

Fig. 3 *a* corresponds to the situation where the standard picture to account for the two segments is well suited (Evans and Ritchie, 1997; Merkel et al., 1999). At low force, the escape from the fundamental 0th state over the outermost barrier is the limiting process. The slope of the first segment is proportional to $k_B T/\hat{x}_2$. For the highest forces (above ~30 pN), the energy of the external barrier is reduced below $\hat{E}_1$ and the deepest bound state remains located at $x_0 = 0$. The process that mostly impedes the unbinding is the overcome of the innermost barrier $\hat{E}_1$ with a rate $k_{0,1}$. The slope of the curve is now larger and proportional to $k_B T/\hat{x}_1$.

Fig. 3 *b* corresponds to an energy landscape for which the above explanation is inappropriate. At low force the unbinding kinetic is controlled by the escape from the fundamental state over the outermost barrier again. But, for pulling forces larger than ~30 pN this outer barrier remains the highest (see inset in Fig. 3 *b*). However the slope of the spectrum increases as in the Fig. 3 *a* case. The reason is that the deepest (and most occupied) bound state is now located

at $x = x_1$ and the presence of the second segment actually witnesses the escape from this intermediate state to the unbound state with a rate $k_{1,2}$. The value of the second slope scales therefore with $k_BT/(\hat{x}_2 - x_1)$. Because the escape rate $k_{1,2}$ in the Fig. 3 *b* case is equal to the escape rate $k_{0,1}$ in the Fig. 3 *a* case, the two spectra in Fig. 3 turn out to be indistinguishable and cannot be a priori associated with one of the two possible landscapes.

Ambiguity in determining the number of barriers

After having shown with the simple example above that ambiguity can exist in determining distances from dynamic force spectra, we show here that even more strikingly it is impossible in general to assess the number of wells and barriers. Again we use a simple example to do so.

Fig. 4 displays two force spectra obtained using Eq. 15. They are both well approximated by a succession of three segments with increasing slopes. Again, the two [log(*r*), *f**] curves are very similar although they are constructed from landscapes that do not even comprise the same number of peaks and wells.

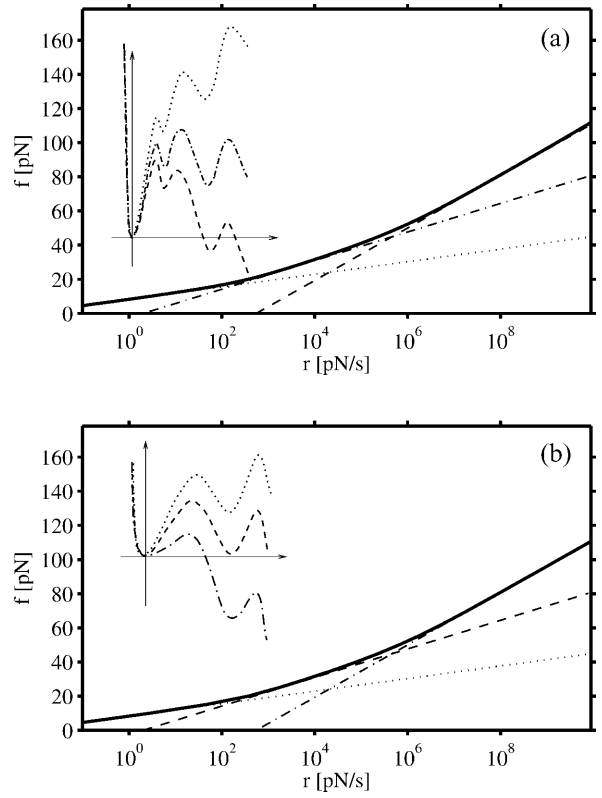

FIGURE 4 Two very similar force spectra corresponding to energy landscapes with different numbers of intermediate wells. The rule of the line styles is the same as in Fig. 3: (*a*) dotted lines: $k_{0,3}$, dash-dotted lines: $k_{0,2}$, dashed lines: $k_{0,1}$. (*b*) dotted lines: $k_{0,2}$, dash-dotted lines: $k_{1,2}$, dashed lines: $k_{0,1}$. Parameter values: (*a*) $(\hat{x}_1, \hat{E}_1) = (0.6\,\text{nm}, 14\,k_BT)$, $(x_1, E_1) = (0.7$ nm, 12 $k_BT)$, $(\hat{x}_2, \hat{E}_2) = (1.1\,\text{nm}, 19\,k_BT)$, $(x_2, E_2) = (2$ nm, 16 $k_BT)$, and $(\hat{x}_3, \hat{E}_3) = (2.5\,\text{nm}, 24\,k_BT)$. (*b*) $(\hat{x}_1, \hat{E}_1) = (1.1\,\text{nm}, 19\,k_BT)$, $(x_1, E_1) = (1.9$ nm, 10 $k_BT)$, and $(\hat{x}_2, \hat{E}_2) = (2.5\,\text{nm}, 24\,k_BT)$.

In Fig. 4 *a* the three segments describe the escape from the same fundamental state over the three distinct energy barriers. The larger the pulling force, the closer the limiting barrier to the fundamental state (see inset in Fig. 4 *a*).

In Fig. 4 *b*, the landscape consists of only two barriers. However, the force spectrum reveals that three different escape processes can limit the unbinding kinetic. At low forces $(f \lesssim 50\,\text{pN})$, the two observed linear segments result from the escape form the fundamental state over the two peaks at $\hat{x}_1$ and $\hat{x}_2$, respectively. Conversely, at high forces it is the escape from the deeply lowered intermediate state over the outer barrier that determines the escape rate (see inset drawing with dash-dotted line in Fig. 4 *b*). With the chosen parameters the effective rates $k_{0,3}$, $k_{0,2}$, and $k_{0,1}$ in the Fig. 4 *a* case correspond respectively to $k_{0,2}$, $k_{0,1}$, and $k_{1,2}$ in the Fig. 4 *b* case. Thus the two plots are indistinguishable and cannot be used to predict the number of barriers along the 1D escape path.

In conclusion of this subsection, we suggest great care in inferring features of the underlying energy landscape from dynamic force spectroscopy experiment. Our generalized equation may be helpful in dealing with the corresponding ambiguity as it allows (with some work) to generate various landscapes that can account for the observed data, whereas Eq. 8 can only yield a single set of parameters (e.g., those used for the plots in Figs. 3 *a* and 4 *a*).

BEYOND THE SINGLE ESCAPE RATE APPROXIMATION: MULTIMODAL UNBINDING FORCE DISTRIBUTIONS

Up to this point we have been considering a generalized theory in which the DBFS approximation is dropped, but the unbinding is still approximated as a simple first-order escape process. Indeed, the validity of Eq. 15 relies on the assumption that at any moment the distribution of the populations of the bound states can be well approximated by the distribution corresponding to a homogeneous stationary current.

This is, however, not always the case. As we stated earlier, the sum of the $1/k_{i,j}(f)$ terms in Eq. 14 is dominated by the smallest effective rate constant $k_{i',j'}(f)$ corresponding to the slowest effective transition. A consequence of this is that all the bound states located to the left of barrier j' are close to equilibrium (because of the slow outflow over barrier j'), and the population of any state located to the right is negligible (because they practically belong to the unbound state). Now, if the slowest transition rate changes from $k_{i',j'}(f)$ to $k_{i'',j''}(f)$ as the loading force f is increased, and if $j'' < j'$, then a considerable population might remain in the intermediate bound states between the new and the old limiting barriers, j'' and j', respectively. This residual population is incompatible with the new stationary current dominated by $k_{i'',j''}(f)$, and must escape in a different way, yielding a secondary maximum of the unbinding force distribution (see Fig. 5, *b* and *c*).

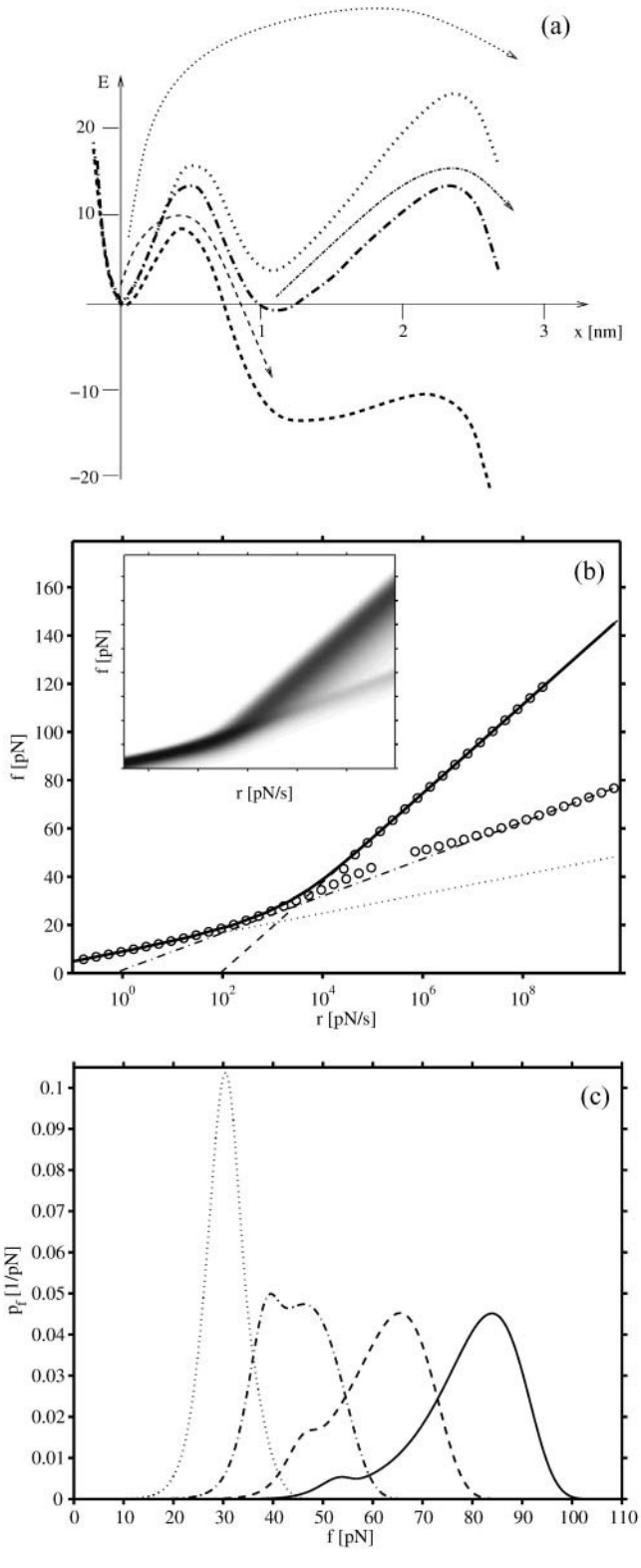

FIGURE 5 A scenario that yields a multimodal unbinding force distribution. (*a*) Three snapshots of the energy landscape for the pulling forces: $f = 0$ pN (*dotted line*), $f = 18$ pN (*dash-dotted line*), and $f = 60$ pN (*dashed line*). The three arrows indicate the corresponding most difficult transitions. Parameters values: $(\hat{x}_1, \hat{E}_1) = (0.5\,\text{nm}, 16\,k_BT)$, $(x_1, E_1) = (1.1\,\text{nm}, 4\,k_BT)$, and $(\hat{x}_2, \hat{E}_2) = (2.3\,\text{nm}, 24\,k_BT)$. (*b*) Force spectrum (*solid line*) associated with the landscape described in *a* plotted using Eq. 15. The full probability density $p_f(f)$ for unbinding at force f is plotted in grayscale in the inset. It has been obtained by following the procedure described in Bartolo et al. (2002). The circles in the main plot represent the local maxima of the distribution. (*c*) The unbinding force distribution $p_f(f)$ for four different values of the loading rate: $r = 3 \times 10^3$, 3×10^4, 3×10^5, and 3×10^6 pN/s from left to right.

The escape of the majority of the population (located to the left of the new limiting barrier j'') can still be characterized by Eq. 14 of our generalized theory. On the other hand, we have to slightly modify this formula to describe the escape of the residual population (trapped between the new and old limiting barriers). Because j'' is the limiting barrier now, almost the entire residual population can escape without ever jumping backward over barrier j''. Therefore, for the residual population we can consider barrier j'' as a reflecting boundary, and describe the escape by our general theory in this modified potential. Eq. 14, e.g., changes accordingly:

$$\tau(f) = \sum_{i=j''}^{N-1} \sum_{j=i+1}^{N} \frac{1}{k_{i,j}(f)} = \sum_{i=j''}^{N-1} \sum_{j=i+1}^{N} \frac{e^{-f\Delta x_{i,j}/k_BT}}{k_{i,j}(0)}. \qquad (16)$$

Consequently, the absolute maximum of the unbinding force distribution always follows the upper envelope of the $N(N + 1)/2$ lines, however, some secondary maxima might also appear at lower forces, which follow the upper envelope of only a subset of the lines (comprising $(N - j'')(N - j'' + 1)/2$ elements). Such secondary maxima of a multimodal force distribution give important information on the internal structure of the energy landscape of the unbinding path, and make the determination of the number and positions of the energy wells and barriers less ambiguous. It is actually a nice achievement of our generalized theory to be able to make sense of the segments of secondary maxima in a unique frame for fitting parameters (see, e.g., Fig. 5, where the segment corresponding to the secondary maximum corresponds to the transition from the intermediate bound state (1) over the rightmost barrier (2), a step neglected in the DBFS approximation). The possibility of a bimodal distribution for the case of a two-state system has already been reported by Strunz et al. (2000), and our description systematizes and generalizes their findings.

To provide a simple illustration for the somewhat formal discussion above, we also focus on a system consisting of two bound states, as depicted in Fig. 5 *a*. Increasing the force, the limiting transition rate changes from $k_{0,2}$ to $k_{1,2}$ and then to $k_{0,1}$. In the range of the loading rate r between $\sim 10^4$ and 10^5 pN/s the intermediate bound state (1) has enough time to accumulate a large population, which is then flushed by the $k_{1,2}$ transition before the transition $k_{0,1}$ flushes the rest from the fundamental bound state (0). In the range above 10^6 pN/s the intermediate bound state (1) cannot accumulate much of the population, but it still possesses a small fraction of the initial equilibrium distribution, which is again flushed by the $k_{1,2}$ transition first.

Very recently the Evans group actually reported the experimental occurrence of a bimodal force distribution (Evans and Williams, 2002). The corresponding experiment consisted of pulling on ''diC14 PE'' lipids from a bilayer made of ''C18:0/1 PC'' lipids. With the help of our generalized theory, Evans and Williams were able to fit their data and interpret the results in terms of an energy landscape with two barriers (see Ref. 3 in Evans and Williams, 2002).

CONCLUSION

In this article, we have revisited the standard theory used to account for the dynamic response of molecular stickers. Our refined description, valid for an arbitrarily complex one-dimensional energy landscape, has allowed us to highlight several practical consequences of the diversity of the possible unbinding scenarios. For example several markedly different energy landscapes can yield the same rupture force distribution. To resolve this ambiguity other experimental techniques, e.g., flow chamber experiments (Pierres et al., 2002), are then required. We have also identified the physical origin of multimodal unbinding force distributions and shown how their analysis provides information on the unbinding pathways.

This work was supported by the Hungarian National Science Foundation (grant number OTKA F043756) and a Marie Curie European Reintegration Grant (No. 505969).

REFERENCES

Bartolo, D., I. Derényi, and A. Ajdari. 2002. Dynamic response of adhesion complexes: beyond the single path picture. *Phys. Rev. E.* 65:051910.

Evans, E. 1998. Energy landscapes of biomolecular adhesion and receptor anchoring at interfaces explored with dynamic force spectroscopy. *Faraday Discuss.* 111:1–16.

Evans, E. 2001. Probing the relation between force lifetime and chemistry in single molecular bonds. *Annu. Rev. Biophys. Biomol. Struct.* 30:105–128.

Evans, E., and K. Ritchie. 1997. Dynamic strength of molecular adhesion bonds. *Biophys. J.* 72:1541–1555.

Evans, E., and P. Williams. 2002. Dynamic force spectroscopy. *In* Physics of Bio-Molecules and Cells. F. Julicher, P. Ormos, F. David, and H. Flyvbjerg, editors. Springer Verlag, Berlin, Germany. 145–204.

Grubmüller, H., B. Heymann, and P. Tavan. 1996. Ligand binding: molecular mechanics calculation of the streptavidin-biotin rupture force. *Science.* 271:997–999.

Hummer, G., and A. Szabo. 2003. Kinetics from nonequilibrium single-molecule pulling experiments. *Biophys. J.* 85:5–15.

Kellermayer, M. S., S. B. Smith, H. L. Granzier, and C. Bustamante. 1997. Folding-unfolding transitions in single titin molecules. *Science.* 276:1112–1116.

Merkel, R., P. Nassoy, A. Leung, K. Ritchie, and E. Evans. 1999. Energy landscapes of receptor-ligand bonds explored with dynamic force spectroscopy. *Nature.* 397:50–53.

Nishizaka, T., R. Seo, H. Tadakuma, K. Kinosita, and S. Ishiwata. 2000. Characterization of single actomyosin rigor bonds: load dependence of lifetime and mechanical properties. *Biophys. J.* 79:962–974.

Pierres, A., A. M. Benoliel, P. Bongrand, and P. A. van der Merwe. 1996. Determination of the lifetime and force dependence of interactions of single bonds between surface-attached CD2 and CD48 adhesion molecules. *Proc. Natl. Acad. Sci. USA.* 93:15114–15118.

Pierres, A., D. Touchard, A.-M. Benoliel, and P. Bongrand. 2002. Dissecting steptavidin-biotin interaction with laminar flow chamber. *Biophys. J.* 82:3214–3223.

Poirier, M. G., A. Nemani, P. Gupta, S. Eroglu, and J. F. Marko. 2001. Probing chromosome structure with dynamic force relaxation. *Phys. Rev. Lett.* 86:360–363.

Rief, M., M. Gautel, F. Oesterhelt, J. M. Fernandez, and H. E. Gaub. 1997. Reversible unfolding of individual titin immunoglobulin domains by AFM. *Science.* 276:1109–1112.

Seifert, U. 2002. Dynamic strength of adhesion molecules: role of rebinding and self-consistent rates. *Europhys. Lett.* 58:792–798.

Simson, D. A., M. Strigl, M. Hohenadl, and R. Merkel. 1999. Statistical breakage of single protein A-IgG bonds reveals crossover from spontaneous to force-induced bond dissociation. *Phys. Rev. Lett.* 83: 652–655.

Strick, T. R., M.-N. Dessinges, G. Charvin, N. H. Dekker, J.-F. Allemand, D. Bensimon, and V. Croquette. 2003. Stretching of macromolecules and proteins. *Rep. Prog. Phys.* 66:1–45.

Strunz, T., K. Oroszlan, I. Schumakovitch, H.-J. Güntherodt, and M. Hegner. 2000. Model energy landscapes and the force-induced dissociation of ligand-receptor bonds. *Biophys. J.* 79:1206–1212.

Weisel, J. W., H. Shumanz, and R. Litvinov. 2003. Protein protein unbinding induced by force: single-molecule studies. *Curr. Opin. Struct. Biol.* 13:227–235.